N93-30872

EXPERIMENTAL BEHAVIOR OF GRAPHITE-EPOXY Y-STIFFENED SPECIMENS LOADED IN COMPRESSION

P. D. Sydow and M. J. Shuart
NASA Langley Research Center
Hampton, Virginia

ABSTRACT

An experimental investigation of the behavior of graphite-epoxy Y-stiffened specimens loaded in compression is presented. Experimental results are presented for element specimens with a single stiffener and for panel specimens with three stiffeners. Response and failure characteristics of the specimens are described. Effects of impact damage on structural response for both specimen configurations are also presented. Experimental results indicate that impact location may significantly affect the residual strength of the Y-stiffened specimens. The failure results indicate that the critical failure mode is buckling of the stiffener webs for Y-stiffened element specimens and buckling of both stiffener web and stiffener blade for the Y-stiffened panel specimens.

INTRODUCTION

Composite materials provide the aerospace engineer with greater freedom in designing aircraft and spacecraft components and appear to have advantages not exhibited by metals. Realizing the potential long-term advantages of composite structures, such as weight savings and high performance, NASA initiated the Advanced Composites Technology (ACT) Program. An objective of the ACT Program is to investigate advanced design concepts for composite aircraft structures. Such advanced concepts include designs that exploit unique characteristics of composite structures and utilize cost-effective manufacturing procedures using advanced material systems or material forms. Stiffness-tailoring is a well-known example of a unique characteristic for composite structures that can be exploited to obtain structurally efficient composite components. Pultrusion is an example of a potentially cost-effective manufacturing procedure for composite structures. Long prismatic structural elements may be pultruded to decrease costly hand lay-up and assembly efforts. An example of an advanced material system is a low-cost damage-tolerant composite material with high compression strength. Such a material would overcome many of the shortcomings of state-of-the-art material systems, and hence become attractive for many aircraft structures applications. Once the attributes of composite materials and the benefits of advanced concepts are fully understood and demonstrated, composite structures technology will mature to the point of being a key factor in the design of state-of-the-art high performance aircraft.

Advanced concepts for composite structures that take advantage of both structural geometry and stiffness tailoring to enhance structural efficiency are being studied for application to primary aircraft structures such as wing cover panels. Previous design studies for metal structures have shown that a Y-stiffened panel is a highly structurally efficient configuration [1,2]. The Y-stiffener configuration combines the desired torsional rigidity of a closed-section stiffener with the bending stiffness of a simple blade stiffener. A stiffness-tailored composite Y-stiffened panel is more structurally efficient than a similar metal panel, and the composite panel may also be fabricated cost effectively.

The objectives of the present paper are to describe the development of a structurally optimized graphite-epoxy Y-stiffened cover panel concept and to present the results of an experimental study of the behavior of several compression-loaded graphite-epoxy Y-stiffened specimens. Experimental results are presented for specimens with a single stiffener, referred to as Y-stiffened element specimens, and for panels with three stiffeners, referred to as Y-stiffened panel specimens. Response and failure characteristics of the specimens are described. Effects of impact damage on structural response for Y-stiffened element specimens and Y-stiffened panel specimens are also presented.

CONCEPT DEFINITION

The concept of a Y stiffener configuration was first conceived in the late 1940's [1,2] and was referred to as the NACA Y-stiffener. This stiffener is shown in Figure 1a. Design requirements for metal stiffeners included both a high resistance to an overall column-like buckling mode and a high resistance to local buckling modes. The metal NACA Y-stiffener design uses the stiffener cap primarily to satisfy the high column-like buckling load design requirement and uses the web thicknesses as a design parameter to suppress local buckling. Optimized configurations were determined using a graphical technique that plotted a weight index as a function of the average stress resultant for the panel [1].

A composite Y-stiffener is shown in Figure 1b. The optimized design for this stiffener was obtained using the Panel Analysis and Sizing COde, PASCO [3]. The structurally optimized panel was designed to carry a combined loading of N_x =14660 lbs/in., N_y =733 lbs/in., and N_{xy} =1367 lbs/in. where N_x, N_y, and N_{xy} are inplane stress resultants of classical plate theory. This loading condition was assumed to be representative of a high compression-dominated loading for the cover panel of a high-aspect-ratio subsonic commercial transport wing. The design variables used in the structural optimization of this panel were stiffener planform dimensions and thicknesses. Lamina properties used for the structural optimization are given in Table 1. The optimized stiffener of the combined-load panel previously described is the stiffener investigated in the present study. The stacking sequences for this composite stiffener are shown in Figure 2. An important simplification indicated in Figures 1 and 2 is the absence of the stiffener cap on the composite stiffener. The optimization results indicate that the stiffness and load-carrying capacity design requirements can be fulfilled without the stiffener cap by tailoring the stiffnesses of the blade, webs, and skin. This design simplification also illustrates how stiffness tailoring can be used to simplify fabrication requirements on a composite structure.

SPECIMENS, APPARATUS, AND TESTS

Composite Y-stiffened specimens were fabricated from a commercially available advanced damage-tolerant material system, Hercules IM7/8551-7 graphite-epoxy preimpregnated tape. The tapes were laid to form 24-ply-thick flat laminates for the specimen skins with laminate stacking sequence $[\pm 45/0/\mp 45/0/\pm 45/0/\mp 45/90]_s$. Tapes were also laid on the manufacturing tool as shown in Figure 2 to form halves for the specimen Y-stiffeners. The flanges and webs of the stiffeners are 16-ply-thick laminates with a $[\pm 45/90/\mp 45/90/\pm 45]_s$ stacking sequence. The blade region for the stiffener halves of the

stiffeners are 23-ply-thick laminates having a $[+45/0_4/-45/0_3/+45/0/\bar{0}]_s$ stacking sequence. Some of the ±45° plies from the flanges and webs are continuous through the blade. All laminates were cured in an autoclave using the manufacturer's recommended procedures. Following cure, the laminates were ultrasonically C-scanned to establish specimen quality. The stiffener halves were bonded together after curing to form the Y-stiffener, and the Y-stiffeners were subsequently bonded to the specimen skins. Hysol EA 934 adhesive was used for all bonding. Bond lines were controlled using 0.005-in.-diameter glass beads.

Typical specimens used in this study are shown in Figure 3. The Y-stiffened element specimen consists of a 20-in.-long by 5.78-in.-wide skin and a single stiffener as shown in Figure 3a. The Y-stiffened panel specimen consists of a 20-in.-long by 17.34-in.-wide skin and three evenly spaced stiffeners as shown in Figure 3b. The specimen ends were secured in a potting material used to introduce load into the structure. The specimen ends were inserted approximately one inch into the potting material, making the effective test section of the specimen approximately 18 inches long. The loaded ends of the specimens were machined flat and parallel to permit uniform compressive end-shortening. The unstiffened side of the skin of each specimen was painted white so that a moire-fringe technique could be used to detect and monitor any out-of-plane deformations during testing. Three element specimens and two panel specimens were fabricated and tested. Stiffened element specimens were designated NY1 through NY3, and stiffened panel specimens were designated NYP1 and NYP2. The specimens were loaded quasi-statically in uniform axial compression to failure using a 300-kip-capacity hydraulic testing machine. The unloaded edges of the skins were simply supported to prevent the specimens from buckling as a column.

A procedure for impacting graphite-epoxy components described in reference 4 was used in the current investigation. Aluminum spheres 0.50 in. in diameter were used as projectiles. These spheres were propelled by a compressed-air gun equipped with an electronic detector to measure projectile speed. All projectile speeds in this study were approximately 550 ft/sec. which corresponds to an impact energy of approximately 27.5 ft-lbs. A schematic of the air gun and a description of its operation are given in reference 4.

Impact sites for specimens in this study are shown in Figure 4. Y-stiffened element specimens NY2 and NY3 were subjected to impact damage prior to testing. Specimen NY2 was impacted at two locations on the unstiffened side of the skin opposite the attachment flanges. The first impact site was located at one-quarter of the test section length, and the second impact site was located at the midpoint of the test section length as shown in Figure 4a (indicated by locations 1a and 1b in Figure 4a). Specimen NY3 was impacted once at the midpoint of the test section length on the blade in the vicinity of the transition region of the web and the blade as shown in Figure 4a (indicated by location 2 in Figure 4a).

Y-stiffened panel NYP2 was subjected to impact damage. Specimen NYP2 was impacted at two locations on the unstiffened side of the skin opposite of the center stiffener attachment flanges prior to testing. The first impact site was located at one-quarter of the test section length, and the second impact site was located at the midpoint of the test section length as shown in Figure 4b (indicated by locations 1a and 1b in Figure 4b). This panel was loaded to a 0.006 in./in. strain level and then unloaded with no visible signs of damage apart from the local delaminations at the sites of impact. Specimen NYP2 was then

impacted at the midpoint of the central blade in the vicinity of the transition region of the web and the blade and loaded to failure (direction of impact was at the minimum angle that would accommodate the compressed-air gun).

The specimens were instrumented with electrical resistance strain gages applied to the flanges, webs, and blades of the Y-stiffened elements and to the skin, webs, and blades of the Y-stiffened panels. Direct-current differential transformers were used to measure specimen end-shortening and out-of-plane displacements. Electrical signals from the instrumentation and the corresponding applied loads were electronically recorded at regular time intervals during the test.

RESULTS AND DISCUSSION

Y-Stiffened Element Specimens

Curves of normalized load versus end-shortening are presented in Figure 5 for the three Y-stiffened element specimens. The applied load P is normalized by the membrane stiffness EA and the end-shortening d is normalized by the specimen length L. This normalized end-shortening d/L is a measure of the specimen's average axial strain. The filled circles appearing in the figure indicate specimen failure.

These normalized load-shortening results appear nearly linear up to a d/L of approximately 0.004 in./in. The slight deviation from a linear response may be attributed to initial geometric imperfections. Specimen NY1 failed at 93.0 kips and an average strain of 0.0096 in./in. Specimen NY2, which was impacted on the unstiffened side of the skin opposite the attachment flanges, failed at 74.3 kips and an average strain of 0.0075 in./in. Specimen NY3, which was impacted near the web-blade interface, failed at 50.1 kips and an average strain of 0.0051 in./in. The failure loads for damaged specimens NY2 and NY3 are 20 percent lower and 46 percent lower, respectively, than the failure load for the undamaged specimen NY1. The effects of impact damage on element specimen failure are discussed below.

The results obtained from strain gages placed on the Y-stiffened element specimens are shown in Figures 6-8. These results were obtained from strain gages located on each specimen as shown in Figures 6a, 7a, and 8a. The circle and square symbols are used in Figures 6-8 to distinguish between individual gages and represent specimen failure. Strain gage results for the undamaged specimen NY1 are presented in Figure 6. The axial strain obtained from back-to-back gages located on the skin-flange region is shown in Figure 6b as a function of the applied load. The strain results presented in this figure exhibit slightly nonlinear behavior similar to the corresponding load-shortening behavior. No strain reversal is observed. Thus these results indicate that no bending or buckling occurred in the skin-flange region during the test. The axial (parallel to the load direction) and the transverse (perpendicular to the load direction) strain in the webs are shown in Figure 6c as a function of the applied load. Axial strains in each specimen web are shown for gage location B1 indicated in Figure 6a, and these strains are always compressive. Transverse strains in each web are shown for gage location B2, and these strains are always tensile. The axial strain results for the webs are similar to the axial strain results for the skin-flange region (Figure 6b). The transverse strain results for the webs show the onset of strain reversal indicating that the webs slightly bend or begin to buckle prior to failure. Axial strain results for the blade are presented in Figure 6d. These results are similar to the axial strain results for the skin-flange region and the web.

Strain gage results for the impact damaged element specimen NY2 are presented in Figure 7. The axial strain from back-to-back strain gages located on the skin-flange region is shown in Figure 7b as a function of applied load. The slight differences in the back-to-back strains for a given load level indicate that local bending or buckling may be initiating. The axial and transverse strains in the webs are shown in Figure 7c as a function of the applied load. The compressive axial strain behavior is linear to failure for one gage and nonlinear for the other gage. The nonlinear strain behavior indicates bending of the web. The slight strain reversal observed for the tensile transverse strain results suggests that the webs buckle just prior to failure. The web transverse strain behavior for the damaged specimen is similar to the web transverse strain behavior for the undamaged specimen NY1, but the failure strain for the damaged specimen is less than the failure strain for the undamaged specimen. Axial strain results for the blade of specimen NY2 are presented in Figure 7d. These results are similar to the axial strain results for the skin-flange region of this specimen. All failure strains on Figure 7 for damaged specimen NY2 are less than the corresponding failure strains on Figure 6 for undamaged specimen NY1. However, the average failure strain for damaged specimen NY2 is greater than 0.0075 in./in. indicating good residual strength in spite of impact damage at the skin-flange region. Good residual strength is defined in this study as average failure strains greater than or equal to 0.006 in./in., in spite of the presence of impact damage.

Strain gage results for the impact damaged element specimen NY3 are presented in Figure 8. The gage locations and orientations are shown in Figure 8a. The axial strain from back-to-back strain gages located on the skin-flange region is shown in Figure 8b as a function of applied load. These strain results are approximately linear to failure, and no strain reversal is observed. The axial and transverse strains in the webs are shown in Figure 8c as a function of the applied load. The compressive axial strain behavior is linear to failure for one web and nonlinear for the other web. The nonlinear behavior indicates bending of this web that is located adjacent to the impact damaged region. The strain reversal observed for the tensile transverse strain results indicates that these webs buckled prior to failure. The axial and transverse strain behavior of the webs of the damaged specimen NY3 is similar to the strain behavior for the damaged specimen NY2. Axial strain results for the blade of specimen NY3 are presented in Figure 8d. The strain reversal observed for these axial strains indicates that the blade buckles prior to failure. All failure strains on Figure 8 for specimen NY3 are less than the corresponding failure strains on Figure 7 for specimen NY2. These failure strain data, failure load data, and global failure strain results for specimens NY2 and NY3 indicate that, for the same impact energy, impact damage at the blade-web interface degrades the structural response of this Y-stiffener configuration more than impact damage at the skin-flange region. The average failure strain for damaged specimen NY3 is approximately 0.005 in./in. indicating marginal residual strength for this specimen with impact damage at the blade-web interface.

The dominant response that initiates failure of these Y-stiffened element specimens is web buckling. Web buckling is a significant design consideration for Y stiffeners since the webs support the blade, and the blade is the primary load-carrying member for this configuration. All three specimens have web strain data that indicate web buckling prior to failure. No buckling was observed from the moire fringe pattern during the element specimen tests indicating that the specimen skin does not buckle. Blade buckling, as indicated by strain gage reversal, only occurs for the specimen impacted at the blade-web intersection. Web buckling may also contribute to the debonding of the adhesively bonded halves of these Y-stiffener blades. A typical failed element specimen and a close-up of the failure region are shown in Figure 9.

Y-Stiffened Panel Specimens

Curves of normalized-load versus end-shortening results are presented in Figure 10 for the two Y-stiffened panel specimens. For the panels, the applied load P is also normalized by the membrane stiffness EA and the end-shortening d is also normalized by the specimen length L. The solid circles indicate failure of the specimen and the open circle indicates termination of the test prior to failure. All results appear nearly linear up to an average strain of approximately 0.005 in./in. The slight deviation from a linear response may be attributed to initial imperfections. Photographs of moire-fringe patterns just prior to specimen failure are shown in Figure 11. The photograph of the first specimen, NYP1, shown in Figure 11a indicates that the buckle pattern of the skin has five half-waves along the length and two half-waves across the width of the region between the stiffeners of the specimen. Specimen NYP1 failed at 285.2 kips, and an average strain level of 0.0078 in./in. The test of the second test specimen, NYP2, was conducted in two phases. First, NYP2 was impacted at two locations on the unstiffened side of the skin opposite the attachment flanges of the center stiffener, in a similar manner as Y-stiffened element NY2 (see Figure 4b). The panel was then loaded to a 0.006 in./in. average strain level to simulate the ultimate compressive strain level a wing cover panel is expected to experience in flight. The panel did not buckle or fail when loaded to an average strain level of 0.006 in./in. In the next phase of the test, NYP2 was impacted once more. The second impact site was located at the midpoint of the test section length and on the central blade in the vicinity of the transition region of the web and the blade (see Figure 4b). This location was determined to be the critical impact site from the previous tests of Y-stiffened element specimens. The panel was then loaded until the center stiffener failed. The failure load was 137.1 kips and corresponds to an average axial strain of 0.0045 in./in. The photograph of specimen NYP2 in Figure 11b shows that the buckling pattern of the skin has a single half-wave along the length and width of the central region between the outermost stiffeners. This mode shape occurred after the center stiffener separated from the skin but prior to separation of the skin from the remaining stiffeners. Specimen NYP2 failed when the skin debonded from the outer stiffeners at a load of 137.2 kips and an average strain of 0.0057 in./in. The maximum loading for the impact-damaged panel was 48 percent less than the maximum loading for the undamaged panel. The effects of damage on panel specimen failure are discussed below.

The strain gage results for the Y-stiffened panel specimens are shown in Figures 12 and 13. These results were obtained from strain gages located on each specimen as shown in Figures 12a and 13a. The circle and square symbols are used in Figures 12 and 13 to distinguish between individual gages and represent specimen failure. Strain results for the undamaged specimen NYP1 are presented in Figure 12. The axial strain obtained from back-to-back strain gages located on the skin between stiffeners is shown in Figure 12b as a function of the applied load. The results presented in this figure indicate slight nonlinear strain behavior similar to the nonlinear load-shortening behavior shown in Figure 10. No strain gage reversal is observed. These results indicate that a slight amount of bending occurs in this region just prior to failure. The axial and the transverse strain in the webs are shown in Figure 12c as a function of the applied load. Axial strains in each specimen web are shown for location B1, and these strains are always compressive like the axial strains obtained in the webs of the stiffened element specimens. Transverse strains in each web are shown for location B2, and, similarly, these strains are always tensile like the transverse strains found in the webs of the stiffened element specimens. Results of Figures 12b and 12c indicate that the axial strain in the webs is similar to the axial strain in the skin (Figure 12b). The transverse strain results for the webs clearly show strain gage reversal which indicates that the webs buckle prior to failure. Axial strain results for the blade are presented in Figure 12d. These results also show strain gage reversal which indicates buckling of the blade.

Strain gage results for the impact damaged panel specimen NYP2 are presented in Figure 13. These results correspond to the second phase of the test in which the panel was loaded to failure. All results obtained in the first phase of the test are linear and have the same slope as the initial slope of the corresponding load versus strain curves obtained in the second phase of the test. The axial strain obtained in the second phase of the test, from back-to-back strain gages located on the skin between stiffeners, is shown in Figure 13b as a function of applied load. These strain results show only a slight indication of local bending in the skin. The axial and transverse strains in the webs are shown in Figure 13c as a function of the applied load. These compressive axial strain results indicate that buckling of both webs has occurred. The strain gage reversal observed for the tensile transverse strain results occur at a strain level of 0.0005 in./in. and indicates that these webs buckled prior to failure. Axial strain results for the blade of specimen NYP2 are presented in Figure 13d. The strain gage reversal observed for these axial strains indicates that the blade of the impact damaged specimen buckles at a much lower load level than the blade of the undamaged specimen. The significant difference in the strains of the back-to-back strain gages suggests that buckling of the blade may have caused a midplane interlaminar shear failure of the blade. All failure strains on Figure 13 for specimen NYP2 are less than the corresponding failure strains on Figure 12 for specimen NYP1. The average axial failure strain for the damaged specimen NYP2 is approximately 0.0057 in./in., indicating marginal residual strength of this panel subjected to a combined impact at the skin-flange region and at the blade-web interface.

Photographs of the failed panel specimens NYP1 and NYP2 are shown in Figures 14 and 15, respectively. Both specimens failed in the test section of the panel. The damage, as a result of failure, appears to be more severe in specimen NYP1 than in specimen NYP2. This difference is due to the much higher failure load of specimen NYP1. The strain results for these panel specimens indicate that buckling of both the web and blade occurs. These results, however, do not conclusively indicate which element buckles first. The results do reinforce the idea that web buckling and blade buckling are important design considerations for Y-stiffened panels.

CONCLUDING REMARKS

This paper describes an experimental investigation of the behavior of graphite-epoxy Y-stiffened specimens loaded in compression. Response and failure characteristics are presented for specimens with a single stiffener, referred to as Y-stiffened element specimens, and for specimens with three stiffeners, referred to as Y-stiffened panel specimens. Effects of impact damage on structural response for both specimen configurations are discussed.

The results presented in this paper indicate that impact location may significantly affect the residual strength of the Y-stiffened specimens. The element specimen impacted on the unstiffened side of the skin opposite the stiffener flanges had an average failure strain greater than 0.0075 in./in. indicating good residual strength. The element specimen impacted near the blade-web interface had an average failure strain of approximately 0.005 in./in. indicating marginal residual strength. The failure results for the damaged element specimens show that, for the same impact energy, an impact at the blade-web interface degrades the maximum load carrying capacity more than an impact at the skin-flange region. The dominant mechanism that initiates failure for all of the Y-stiffened element specimens is bending or buckling of the webs.

Results are also presented for a damaged panel specimen that was first impacted on the unstiffened side of the skin opposite the stiffener flanges of the center stiffener, and

loaded to a global strain level of 0.006 in./in. After unloading the specimen it was then impacted near the blade-web interface of the center stiffener which resulted in an average failure strain of 0.0057 in./in. indicating marginal residual strength. The dominant mechanism that initiated failure in both of the Y-stiffened panel specimens was a combination of web and blade buckling.

ACKNOWLEDGMENTS

The authors gratefully acknowledge the computer support given by Janice S. Myint for the reduction of the experimental data.

REFERENCES

1. Dow, N. F.; and Hickman, W. A.: Design Charts for Flat Compression Panels Having Longitudinal Extruded Y-Section Stiffeners and Comparison with Panels Having Formed Z-Section Stiffeners. NACA TN 1389, 1947.

2. Dow, N. F.; and Hickman, W. A.: Comparison of the Structural Efficiency of Panels Having Straight-Web and Curved-Web Y-Section Stiffeners. NACA TN 1787, 1949.

3. Anderson, M. S. ; and Stroud, W. J.: General Panel Sizing Computer Code and Its Application to Composite Structural Panels. AIAA Journal, Vol. 17, Aug. 1979, pp. 892-897.

4. Starnes, J. H., Jr.; Rhodes, M. D.; and Williams, J. G.: Effect of Impact Damage and Holes on the Compressive Strength of a Graphite/Epoxy Laminate. Nondestructive Evaluation and Flaw Criticality for Composite Materials, STP 696, R. B. Pipes, ed., American Society for Testing and Materials, 1979, pp. 145-171.

Table 1. Properties for IM7/8551-7A used for structural optimization.

Longitudinal Young's modulus, E_{11}, Msi	20.9
Transverse Young's modulus, E_{22}, Msi	1.5
Shear modulus, G_{12}, Msi	0.72
Poisson's ratio, ν_{12}	0.33
Nominal ply thickness, in.	0.0055

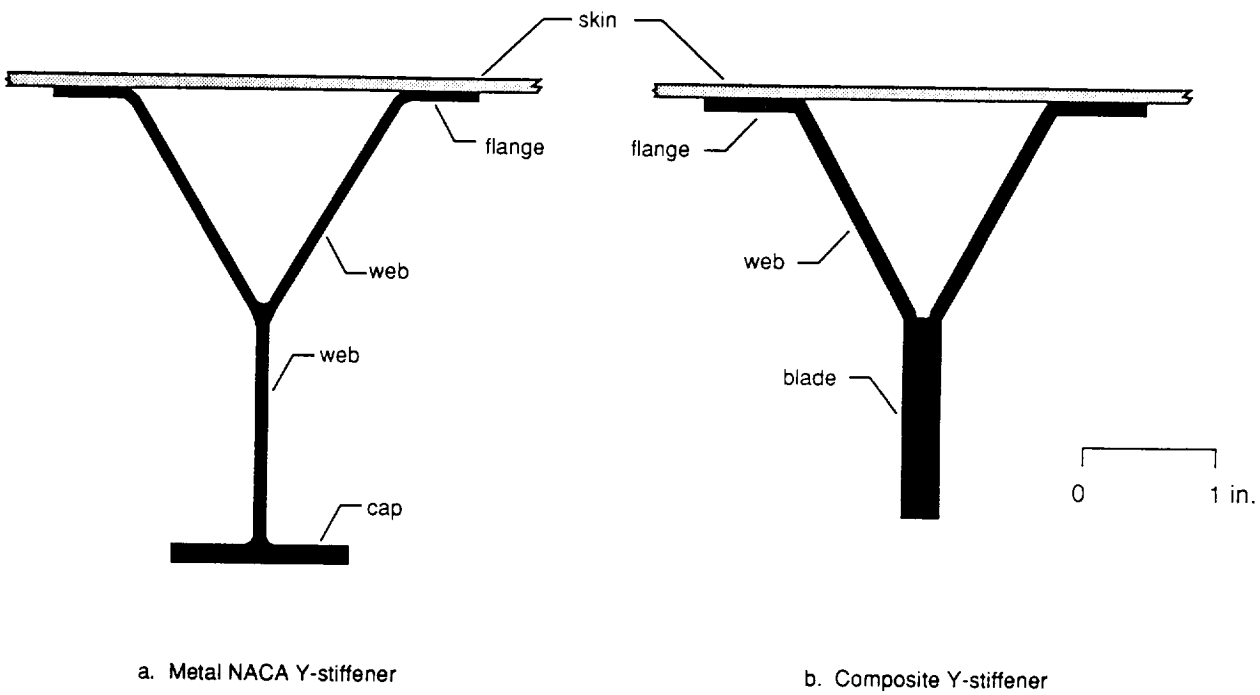

Figure 1. Y-Stiffener Configurations.

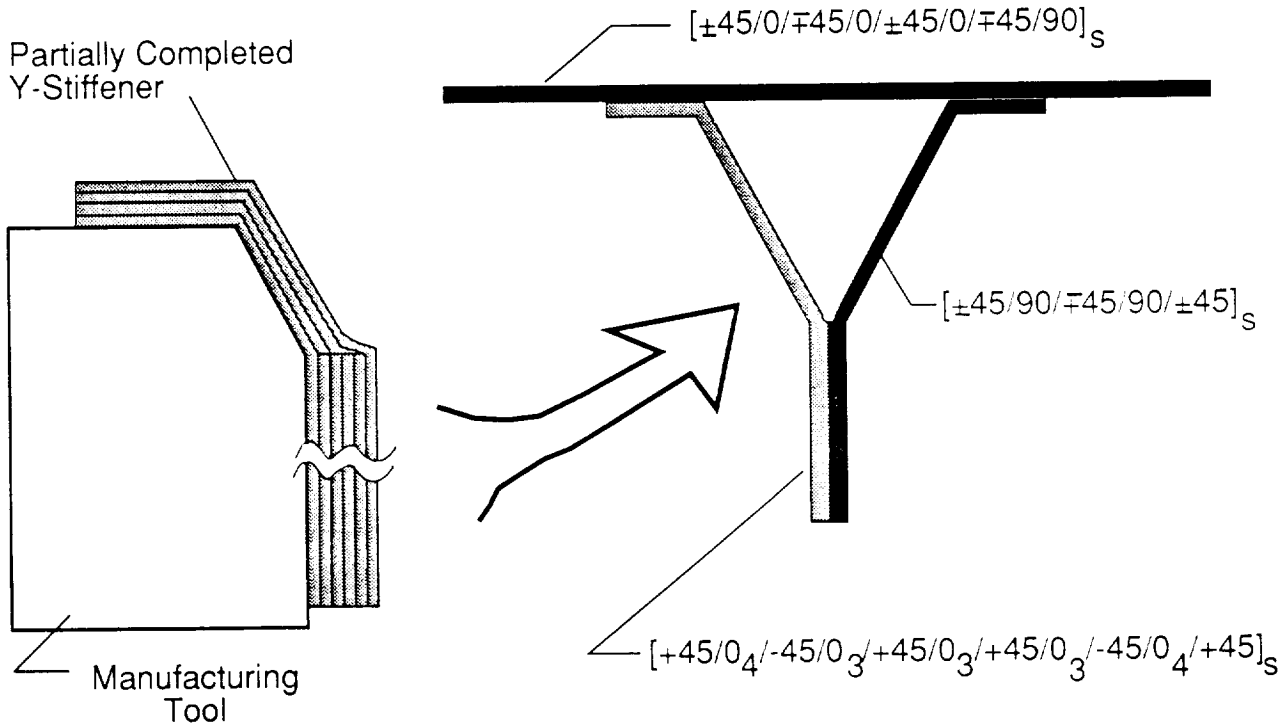

Figure 2. Fabrication of Composite Y-Stiffened Element.

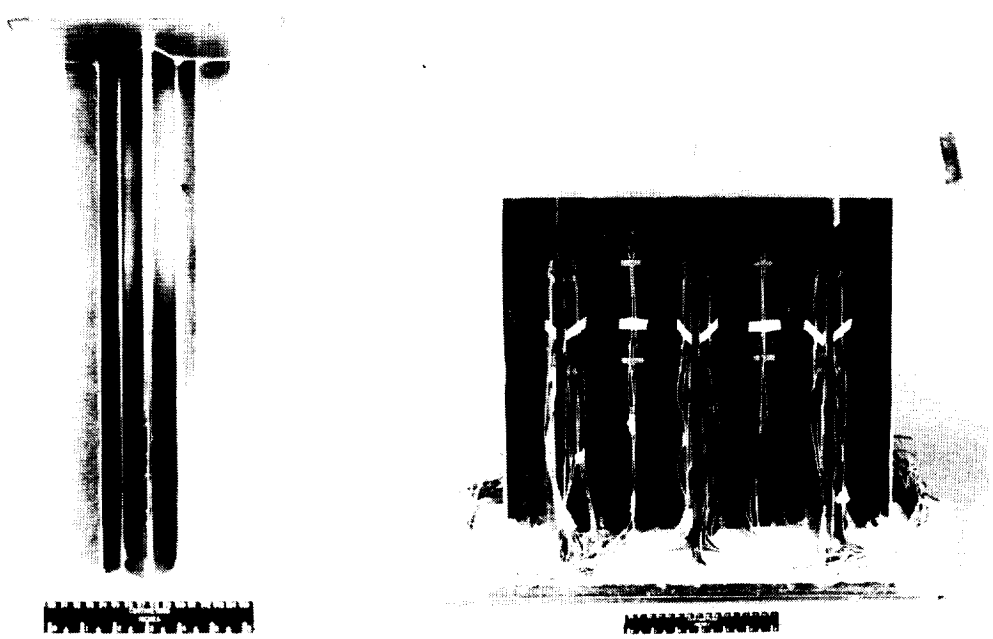

a. Single-stiffener element specimen

b. 3-stiffener panel specimen

Figure 3. Y-stiffened specimens.

ORIGINAL PAGE
BLACK AND WHITE PHOTOGRAPH

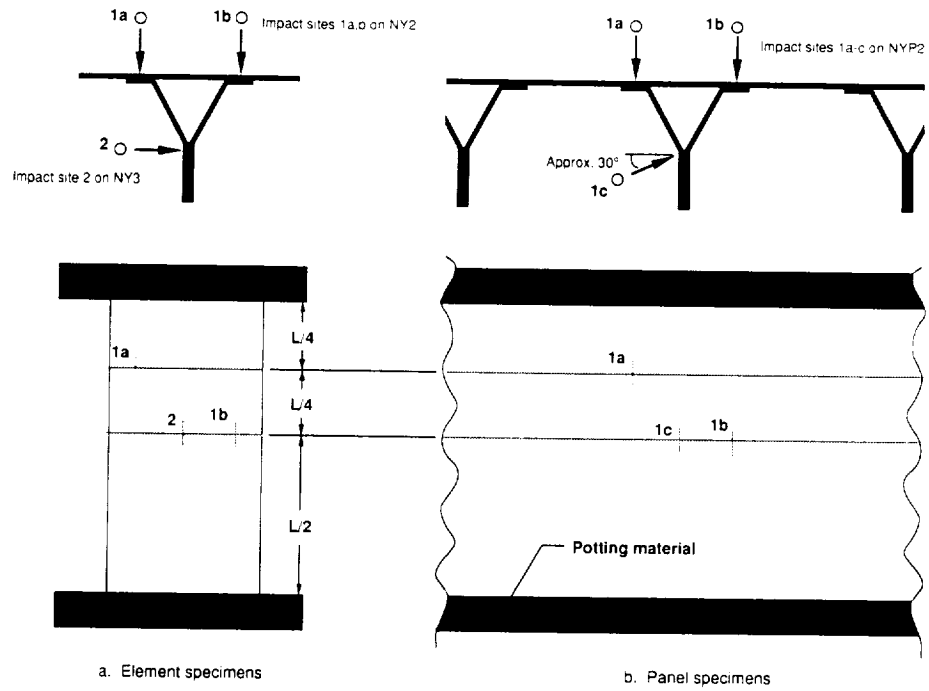

Figure 4. Impact sites for Y-stiffened specimens.

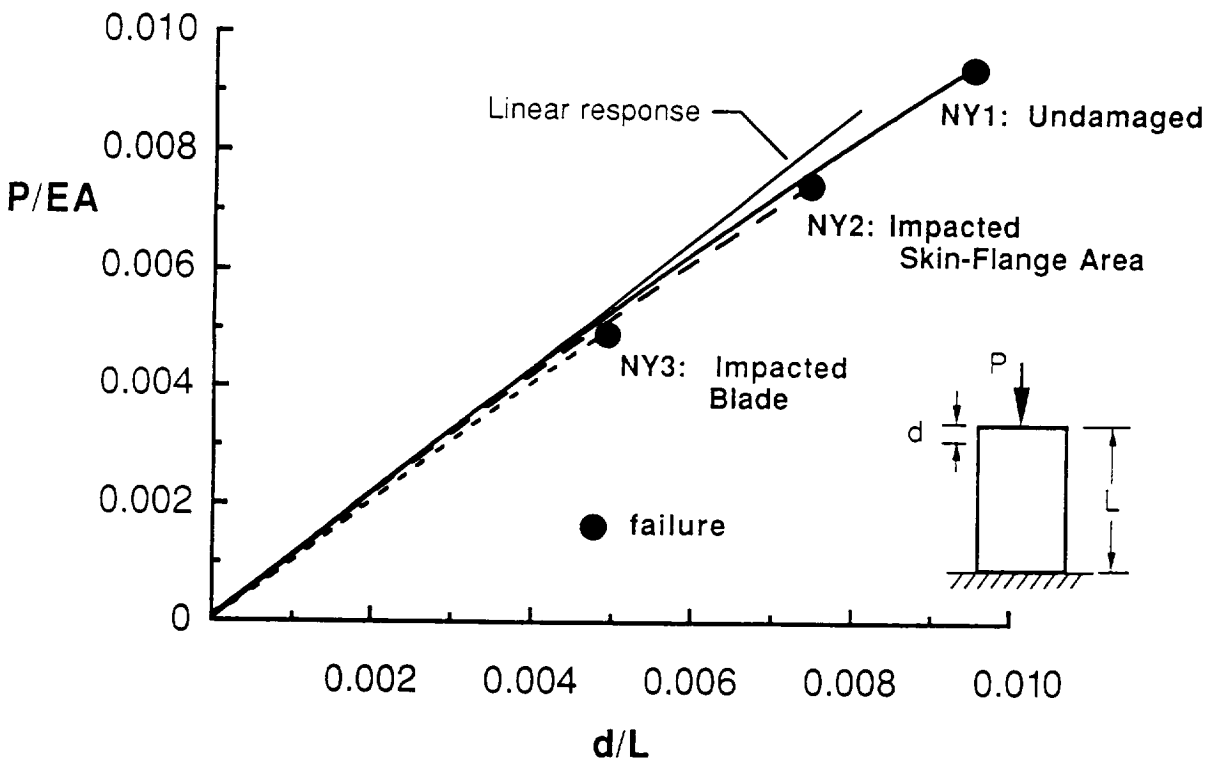

Figure 5. Normalized load versus end-shortening for Y-stiffened element specimens.

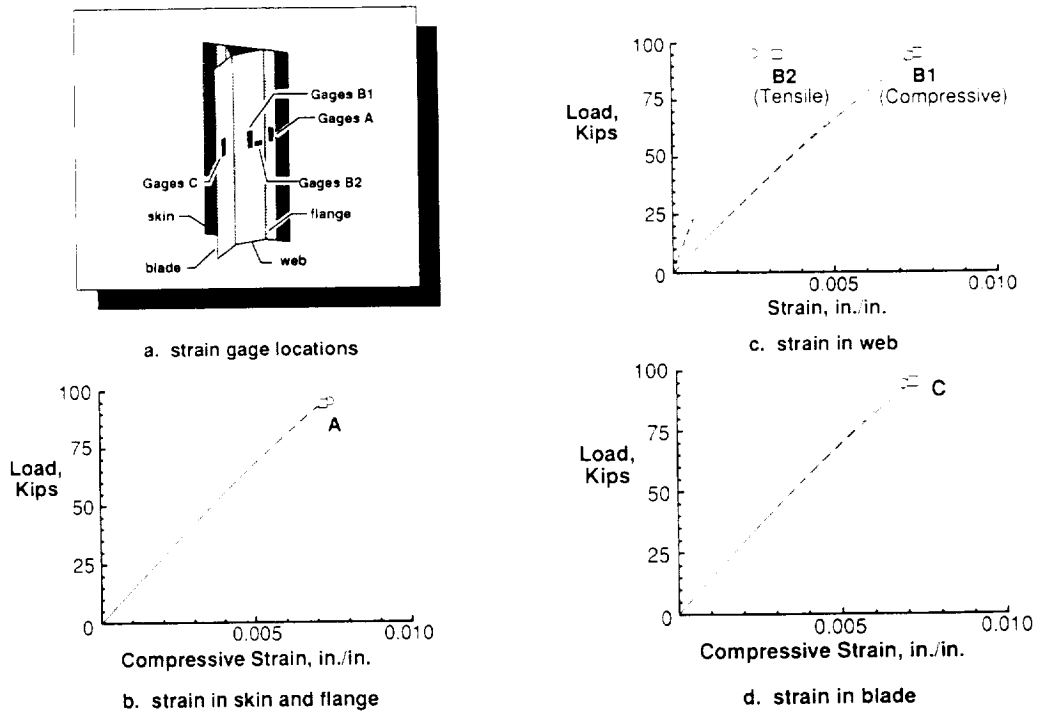

Figure 6. Strain gage results for undamaged element specimen NY1 (square and circular symbols used to distinguish between individual gages).

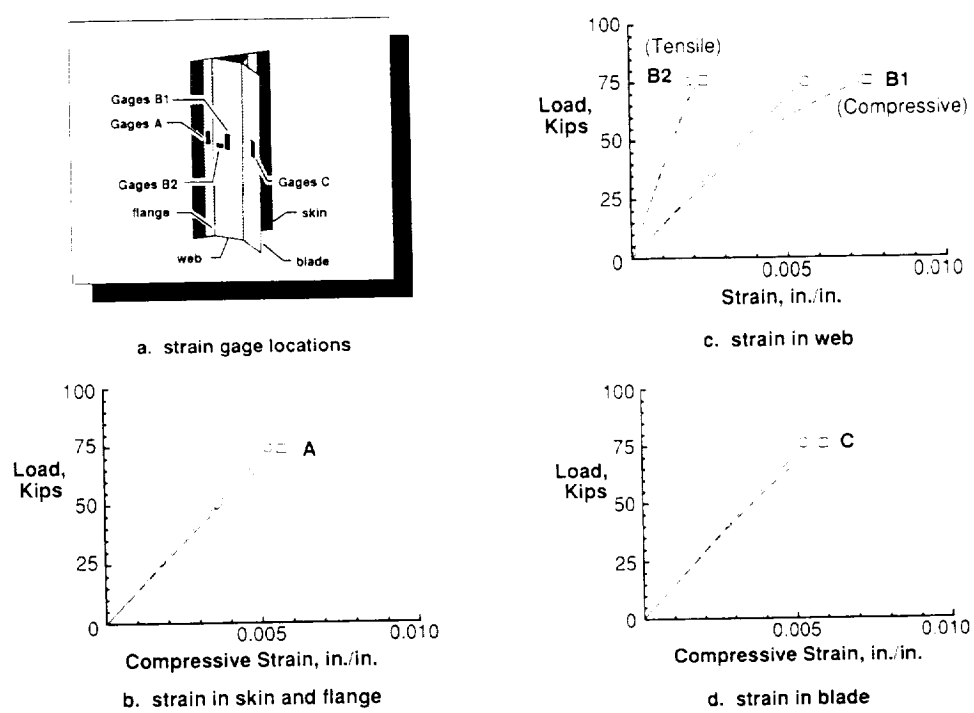

Figure 7. Strain gage results for impact damaged element specimen NY2 (square and circular symbols used to distinguish between individual gages).

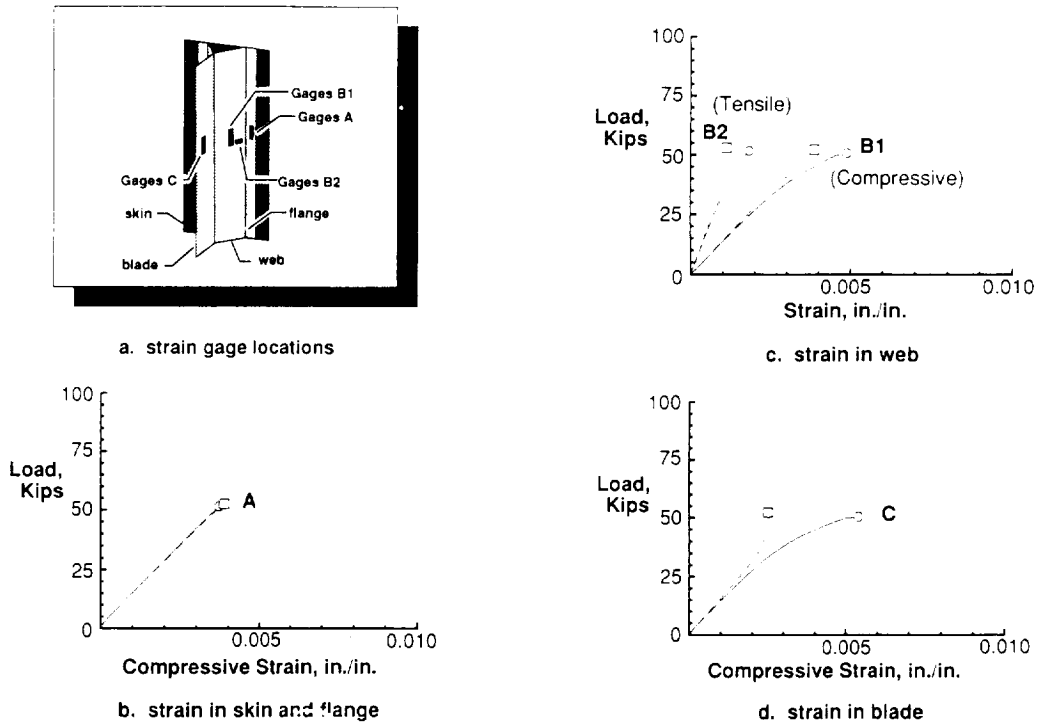

Figure 8. Strain gage results for impact damaged element specimen NY3 (square and circular symbols used to distinguish between individual gages).

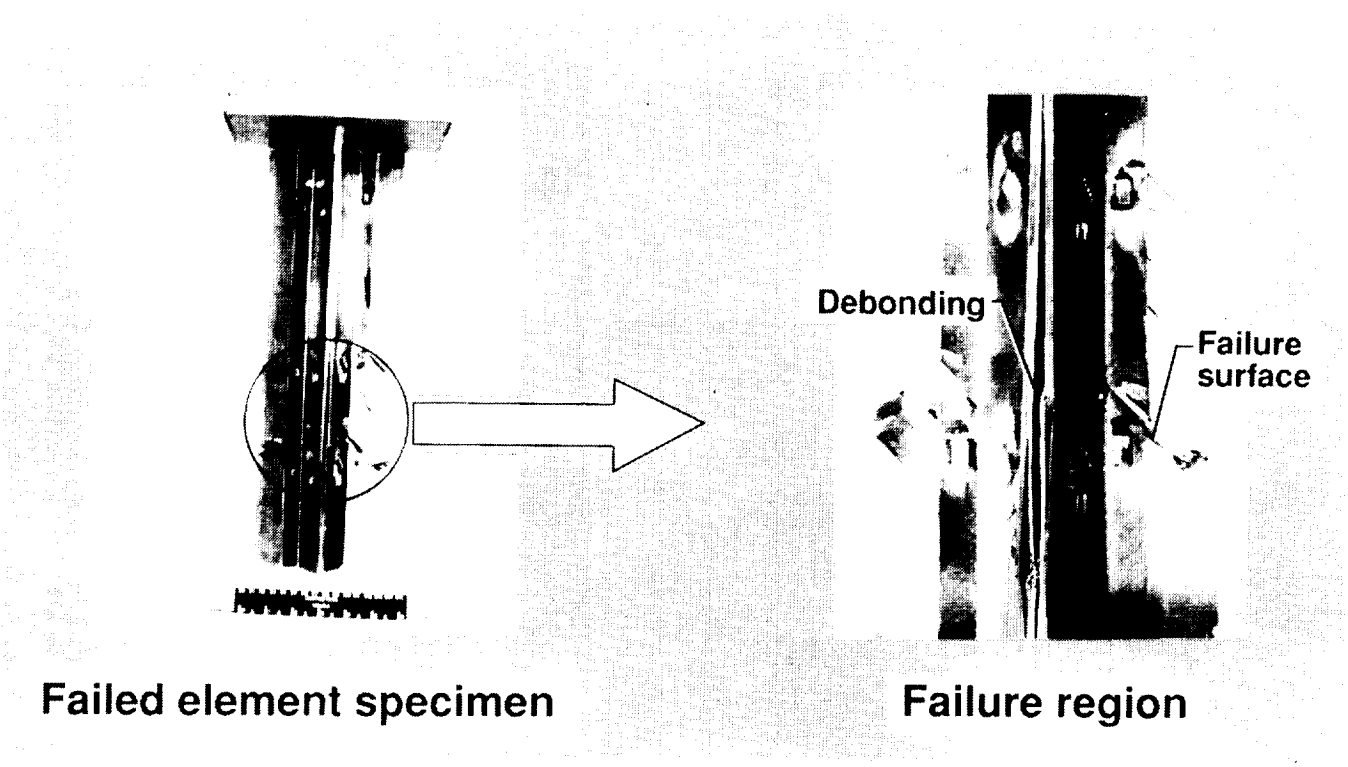

Figure 9. Typical failure of Y-stiffened element specimen.

ORIGINAL PAGE
BLACK AND WHITE PHOTOGRAPH

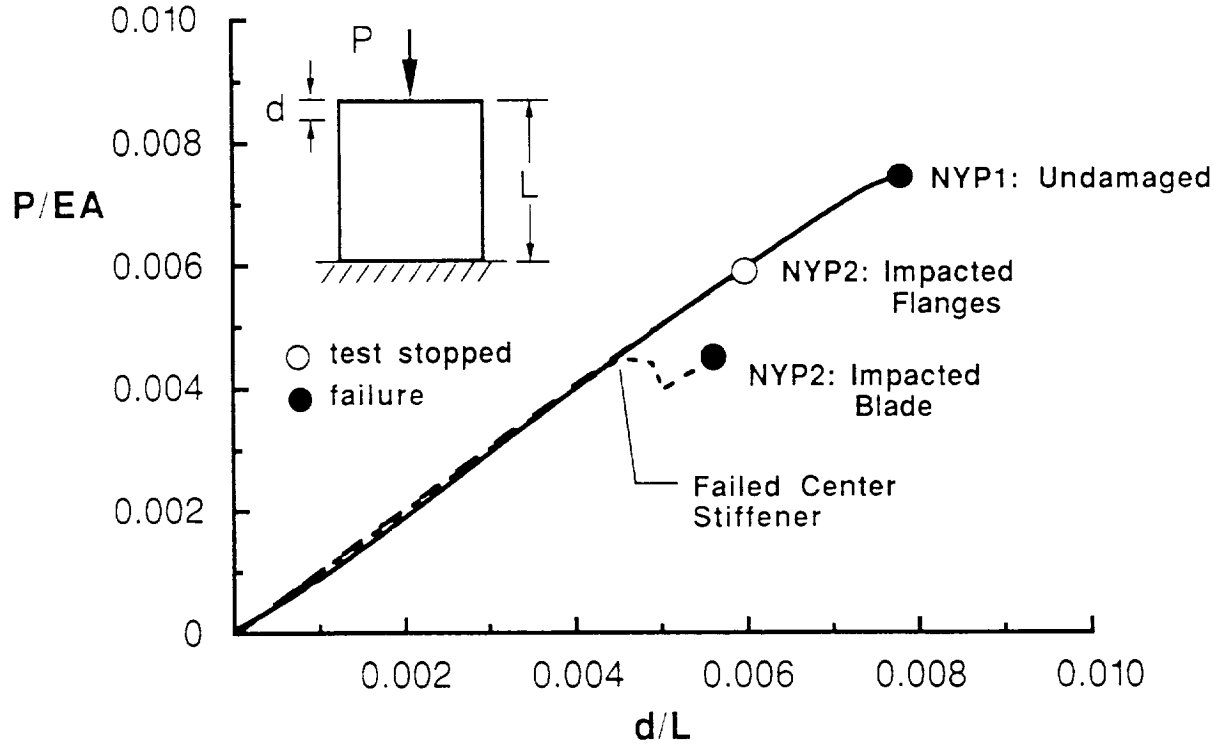

Figure 10. Normalized load versus end-shortening for Y-stiffened panel specimens.

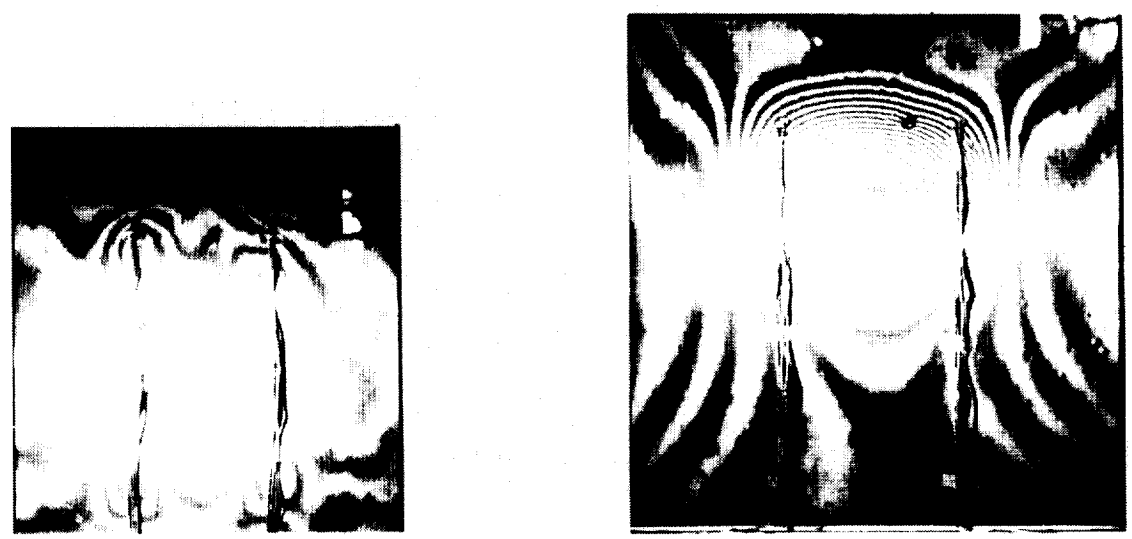

a. Specimen NYP1, P = 283 Kips (P/P_{max} = 0.992)

b. Specimen NYP2, P = 137 Kips (P/P_{max} = 0.998)

Figure 11. Photographs of moire fringe patterns for Y-stiffened panel specimens.

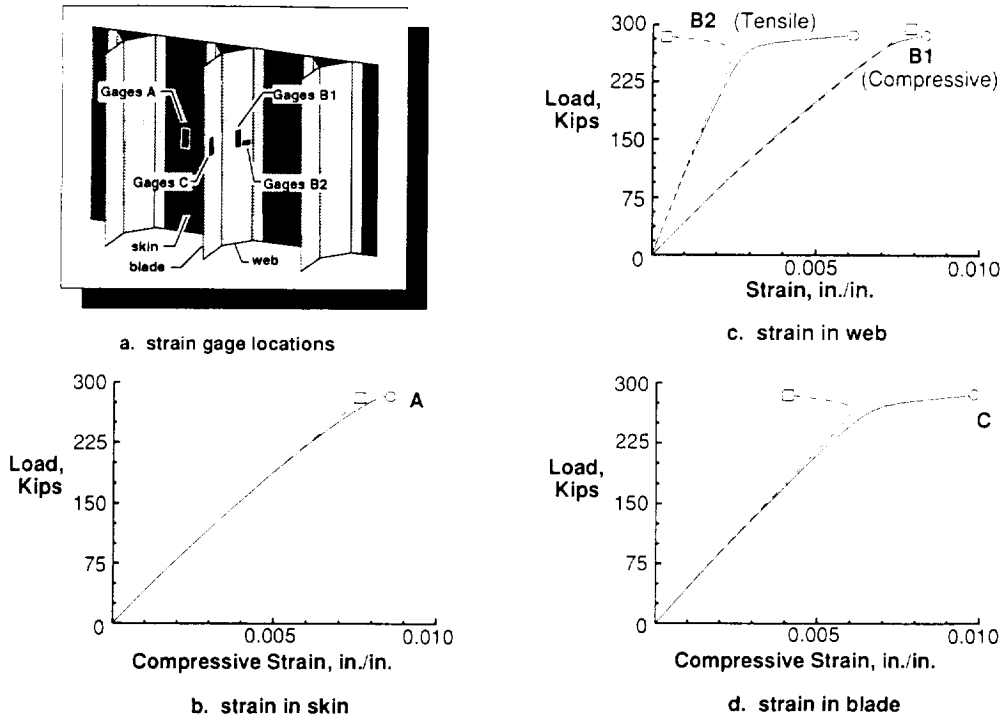

Figure 12. Strain gage results for undamaged panel specimen NYP1 (square and circular symbols used to distinguish between individual gages).

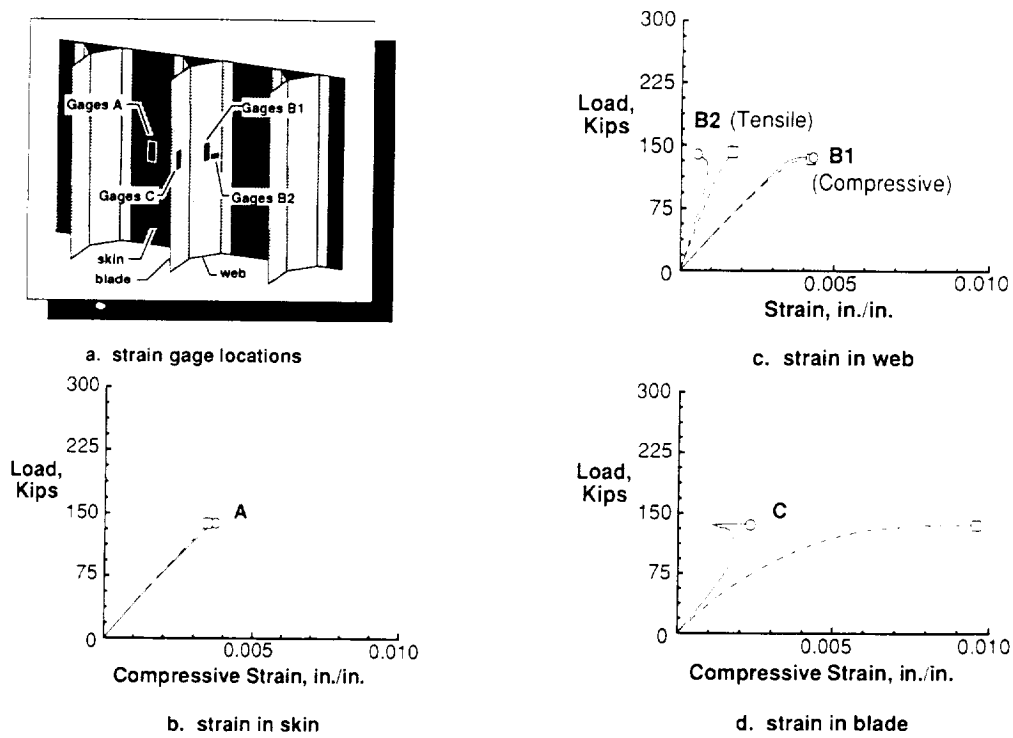

Figure 13. Strain gage results for impact damaged panel specimen NYP2 (square and circular symbols used to distinguish between individual gages).

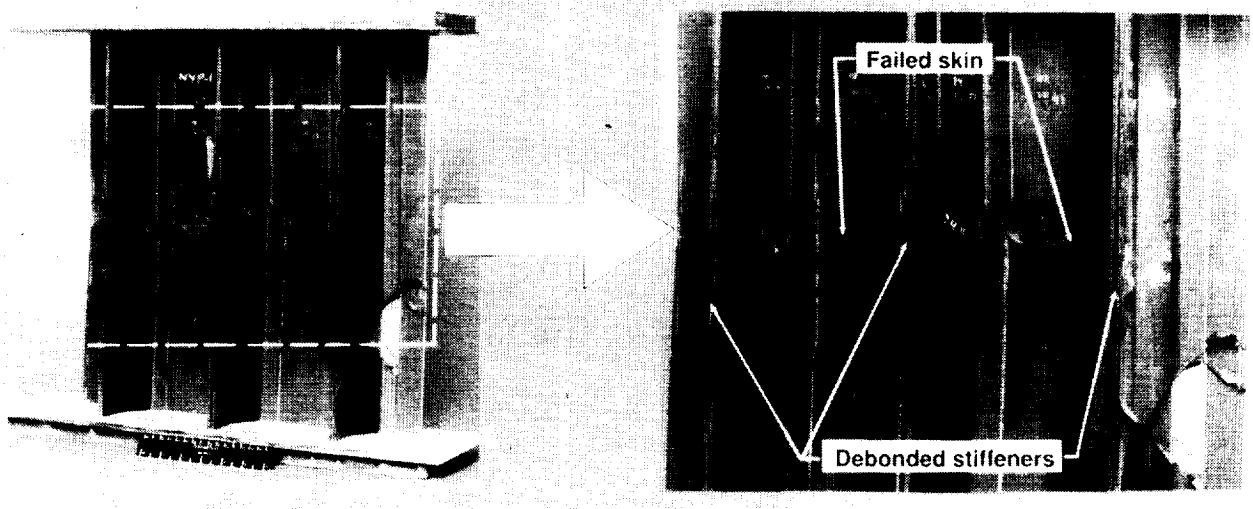

Failed panel specimen NYP1 Failure region

Figure 14. Failure mode of Y-stiffened panel specimen NYP1.

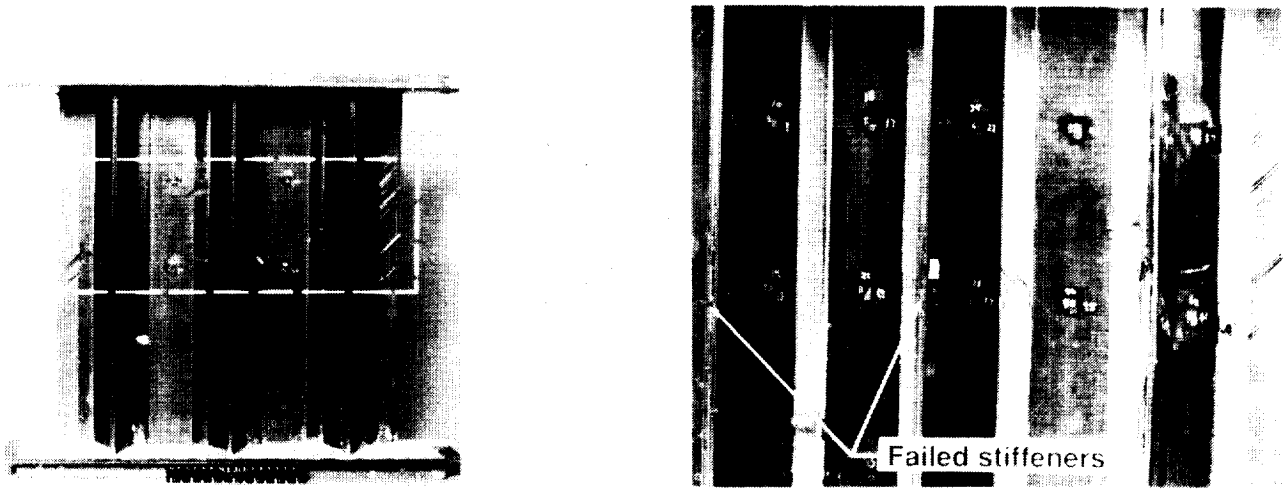

Failed panel specimen NYP2 Failure region

Figure 15. Failure mode of Y-stiffened panel specimen NYP2.